

Article

Seismic Resilience in Critical Infrastructures: A Power Station Preparedness Case Study

Gili Lifshitz Sherzer ¹, Alon Urlainis ¹ , Shani Moyal ² and Igal M. Shohet ^{2,3,*} 

¹ Department of Civil Engineering, Ariel University, Ariel 40700, Israel; gilil@ariel.ac.il (G.L.S.); alonu@ariel.ac.il (A.U.)

² Department of Civil and Environmental Engineering, Ben-Gurion University of the Negev, P.O. Box 653, Beer Sheva 84105, Israel; moyas@post.bgu.ac.il

³ Department of Civil and Construction Engineering, Chaoyang University of Technology, 168, Jifeng E. Rd., Wufeng District, Taichung 41349, Taiwan

* Correspondence: igals@bgu.ac.il; Tel.: +97486479682

Abstract: The role of critical infrastructures in maintaining the functioning of the economy and society and ensuring national security, particularly their durability in delivering essential services during crises, including natural disasters such as earthquakes, is critical. This work introduces an analytical methodology to quantify potential earthquake damage to power stations and evaluate the cost-effectiveness of measures to enhance their seismic resistance. By employing fragility curves and probabilistic risk analyses, this approach provides a structured framework for the comprehensive assessment of risks and the identification of economically practical mitigation strategies. A detailed examination of strategies to protect critical power station components against seismic activity is presented, revealing that a minor investment relative to the overall project budget for earthquake-proofing measures is economically effective. This investment, representing a marginal fraction of 0.5% of the total project expenditure significantly reduces the seismic risk of power station failure by 36%. Reinforcing essential elements, including switching stations, water treatment facilities, and water tanks, is emphasized to ensure their continued operation during and after an earthquake. This research highlights the critical significance of integrating risk assessment with benefit-to-cost analysis in strategic decision-making processes, supporting the prioritization of investments in infrastructure enhancements. These enhancements promise substantial reductions of risks at minimal costs, thus protecting essential services against the impacts of natural disasters. This research contributes to state-of-the-art research in critical infrastructures resilience.

Keywords: critical infrastructures; fragility curves; probabilistic risk analysis; benefit-to-cost analysis; mitigation strategies



Citation: Lifshitz Sherzer, G.; Urlainis, A.; Moyal, S.; Shohet, I.M. Seismic Resilience in Critical Infrastructures: A Power Station Preparedness Case Study. *Appl. Sci.* **2024**, *14*, 3835.

<https://doi.org/10.3390/app14093835>

Academic Editors: Virginio Quaglino, Tommaso D'Antino and Eleonora Bruschi

Received: 11 April 2024

Revised: 26 April 2024

Accepted: 27 April 2024

Published: 30 April 2024



Copyright: © 2024 by the authors. Licensee MDPI, Basel, Switzerland. This article is an open access article distributed under the terms and conditions of the Creative Commons Attribution (CC BY) license (<https://creativecommons.org/licenses/by/4.0/>).

1. Introduction

The impact of natural hazards on critical infrastructure, significantly affecting global economies and communities, is demonstrated by extreme events such as the 2009 floods in Cumbria [1], the Tohoku earthquake and tsunami in 2011 [2], and the 2023 Turkey–Syria earthquake [3]. These occurrences underline the persistent need for enhanced resilience in the design and management of infrastructure systems. Similarly, scour has emerged as a significant factor in bridge failures worldwide. The challenges associated with these hazards are further amplified by the effects of climate change, which leads to more frequent and severe extreme weather events, thus intensifying the risks to critical infrastructures [4]. The threats of multiple hazards, as seen in disasters such as the 2004 Indian ocean earthquake and tsunami and the 2011 Tohoku earthquake and tsunami [2,5], necessitate a robust resilience strategy.

The necessity for resilient infrastructure capable of withstanding, responding to, and adapting to a broad spectrum of hazards, including climate change effects, is a growing

concern for critical infrastructure owners and operators. As defined by Woods (2015) [6], resilience signifies the essential qualities that enable critical infrastructure systems to maintain or enhance their continuous performance amid disruptive events. These events need to span numerous research domains. Yet, the establishment of solid quantitative metrics for the resilience of socio-technical systems and comprehensive standards is still progressing, as indicated by the Lloyd's Register Foundation (2015) [7]. The emphasis on developing resilient cities and critical infrastructures for effective disaster management has intensified, with prevalent methods primarily relying on qualitative analyses and indices, as noted by [8,9]. Yang et al. [10] conducted a comprehensive review on the implementation of resilience assessment for critical infrastructures, highlighting its growing importance in managing urban safety and resilience during crises or disasters. Their findings underscore the need for the establishment of a uniform standard system of indicators to enhance the assessment and improvement of critical infrastructure resilience effectively.

Addressing some of these challenges, the work of Urlainis and Shohet (2022) [11] explores the correlation between economic losses and damage to critical infrastructure, proposing a probabilistic seismic risk mitigation approach. Utilizing Fault Tree Analysis, fragility curves, and the Risk Mitigation to Investment Ratio (RMIR), their methodology aims to strategically prioritize mitigation efforts to protect against seismic threats. Furthermore, Urlainis et al. (2022) [2] highlight the role of critical infrastructures such as hospitals, power stations, and communication centers in ensuring societal and economic stability [2]. They propose a comprehensive multi-hazard risk assessment and management framework, aiming to strengthen the preparedness and resilience of critical infrastructure against a diverse array of natural threats. This approach stresses the necessity of risk assessment and mitigation strategies throughout different sectors to ensure essential services are protected and societal functions remain uninterrupted during natural disasters. Complementing existing methodologies, the seismic fragility assessment framework by Fei et al. (2023) [12] offers a novel perspective by focusing on urban functional spatial units. This approach integrates both structural and functional aspects of urban planning, enhancing traditional resilience assessments by providing a more granular understanding of urban vulnerabilities. This methodology enriches the multi-hazard risk assessment strategies discussed, supporting targeted urban planning efforts crucial for enhancing infrastructure resilience. Furthermore, Mogheisi et al. (2023) [13] emphasize the importance of assessing potential direct and indirect damages to bridges before earthquakes occur. This proactive evaluation enables the implementation of optimal rehabilitation strategies to minimize damage. Such assessments are crucial, as the seismic resilience of urban transportation infrastructure plays a vital role in maintaining functionality in post-disaster scenarios. This study highlights the necessity for continuous updates in seismic risk evaluations and the retrofitting of existing structures to enhance urban infrastructure resilience effectively.

In addition to structural elements, the seismic vulnerability of nonstructural components also demands attention. Rota et al. (2023) [14] underscored the importance of monitoring nonstructural elements in buildings, utilizing accelerometric sensors to identify critical acceleration thresholds. This approach not only predicts potential damage to these elements during seismic events but also facilitates the prioritization of inspection and mitigation actions post-event. Such monitoring is crucial, as these components often constitute a significant portion of the building's capital value and play a vital role in ensuring occupant safety and building functionality during and after earthquakes.

Extending these discussions, current research on seismic resilience provides methodologies for enhancing the robustness and resilience of critical infrastructure in the case of earthquake events [15]. For example, Shafieezadeh and Ivey Burden (2014) [16] introduce a probabilistic framework for scenario-based resilience assessments, emphasizing the importance of preparedness and mitigation planning in the context of harbors. Furthermore, Espinoza et al. (2020) [17] presented an approach that integrated the assessment of risk and resilience, incorporating uncertainty and the time-dependency of the recovery process, demonstrating how retrofitting selective components can notably improve sys-

tem resilience [17]. Capacci and Biondini (2020) offer insights into the life-cycle seismic resilience assessment of aging infrastructure, stressing the long-term impacts of seismic events and the benefits of infrastructure upgrades and retrofitting [18]. Forcellini (2022) [19] highlighted the consideration of interconnected infrastructure systems for analyzing systemic vulnerabilities and resilience enhancement strategies. Rezvani et al. (2024) [20] introduced the Risk-Informed Asset-Centric (RIACT) process, a novel methodology aimed at enhancing urban resilience against earthquakes, particularly assessing the preparedness and recovery capabilities of Portugal's municipalities. This approach utilizes GIS mapping to offer a comprehensive analysis of earthquake risks, highlighting the necessity for tailored resilience strategies across different regions.

In this research, we focus on a comprehensive risk analysis for a gas power station located along the southern coastal region of Israel. The research aims to enhance the station's resilience to seismic activities. The proposed approach begins by thoroughly examining the station's geographical setting and structural design to identify seismic risks and potential threats, including earthquakes, ground amplification, slope stability issues, and soil liquefaction. We then advance to a detailed damage assessment and failure analysis, employing fragility curves to estimate the potential impact of seismic events while considering how different station components interact and depend on one another. Subsequently, our investigation explores various mitigation strategies, such as the anchoring of subcomponents, to enhance the station's seismic resilience. This phase includes a benefit-to-cost analysis (BCA) to confirm the economic feasibility of these strategies. The final phase of the research involves formulating actionable recommendations to improve the station's ability to withstand seismic events. By adopting this detailed approach, one can determine the effectiveness of particular mitigation strategies and establish a comprehensive framework for enhancing the seismic resilience of critical infrastructure, providing valuable guidance for academic researchers and industry practitioners.

This study enriches the existing literature by presenting a comprehensive cost-benefit analysis of seismic mitigation strategies. It identifies potential approaches such as structural retrofitting, estimates the associated implementation costs, and assesses the benefits, focusing mainly on direct loss avoidance and indirect benefits. By determining the probability of seismic events using historical data and forecasts, the study evaluates the economic effectiveness of each strategy through a BCA. Decision trees are used to systematically compare and quantify the benefits and costs, identifying the most cost-effective options. This approach ensures a robust framework for decision making on seismic mitigation measures, emphasizing the financial justification of strategies.

2. Background

2.1. Seismological Risks

In seismic regions worldwide, seismological risks significantly threaten communities, critical infrastructures, and natural landscapes. This study specifically focuses on the Israeli region, highlighting the Great Rift Valley as a notable area of interest due to its significant seismic activity [21]. The Great Rift Valley is an expansive geological rift system from the Beqaa Valley in Lebanon to Mozambique in the south. It forms part of a larger system that encompasses both the Eastern and Western Rift Valleys, shaped by the gradual separation of the Earth's crust, which leads to the creation of fault lines, escarpments, and profound valleys. Beyond its geological significance, the valley is notable for its rich biodiversity and crucial archaeological sites that provide insight into human evolution. This rift system presents a notable earthquake hazard to regions it traverses, including Israel. It influences a distinct movement pattern where the land east of the Jordan River shifts northward while the terrain to the west moves southward. These tectonic activities have progressed slowly, 5 to 10 mm per year over the last 10 to 20 million years. Although Israel is geographically situated in a region with low seismic activity, its history reveals several earthquakes that have resulted in considerable loss of life and damage to structures. The pattern of earthquake occurrence rates along a portion of the Great Rift Valley indicates

that earthquakes with a magnitude of 6 and above, happening in and around Israel, align with a trajectory stretching from the Lebanon Valley to the southern Dead Sea. Figure 1, on the top left, displays a map to determine the epicenters of these earthquakes since 1900, categorized by their intensity. Furthermore, the Carmel Rift is another zone of notable seismic activity from the Carmel region to the Sea of Galilee.

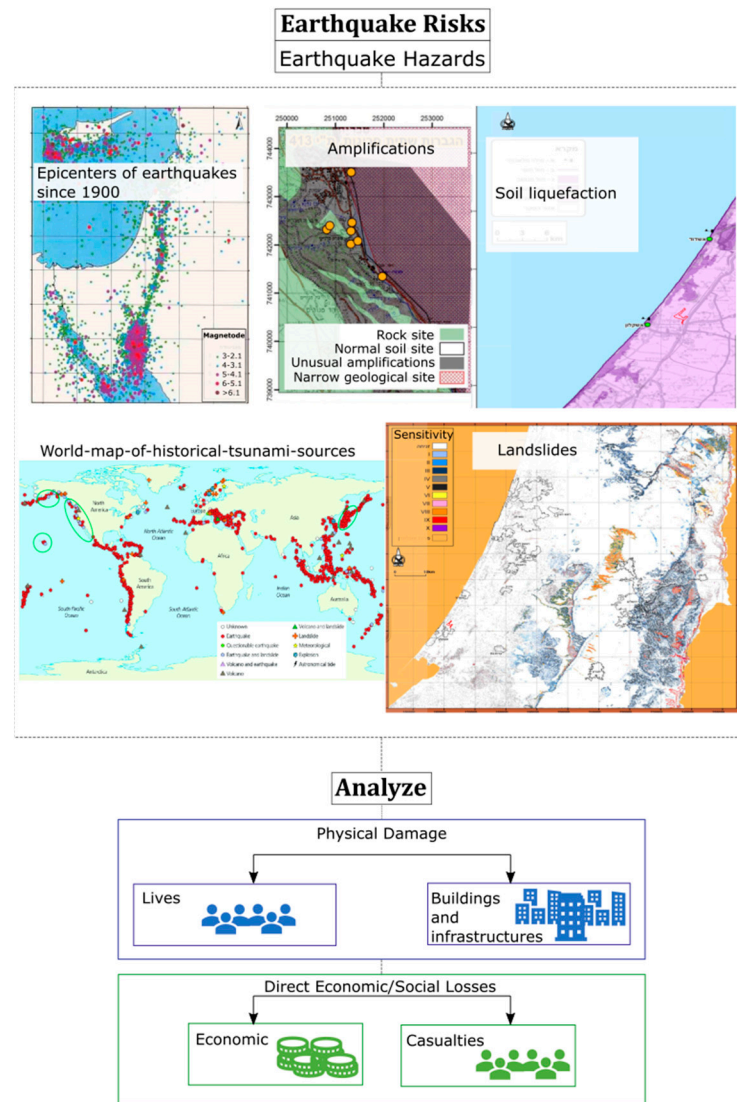


Figure 1. Earthquake hazards analysis.

Seismological centers primarily assess seismic risk, estimating the potential ground motions seismic waves trigger. These potential ground motions are commonly quantified using Peak Ground Acceleration (PGA), which serves as an indicator of the intensity of ground shaking at a site during an earthquake [22]. Such assessments commonly incorporate uncertainty, leading to the inherently probabilistic nature of seismic risk evaluations. The Israeli standard (IS 413) [23,24] accounts for the likelihood of buildings being subjected to significant ground motion (which does not necessarily stem from a major earthquake). It suggests that, if a building is expected to serve its occupants for 50 years, there is a 90% probability that it will not experience ground motions more severe than those prescribed by the standard, given a PGA with a cumulative probability of 10%.

2.2. Secondary Phenomena (Aftershocks and Beyond)

Following an earthquake, secondary events are foreseen, with the nature of these phenomena heavily influenced by the local site conditions. The terrain is susceptible to landslides along slopes in mountainous regions, whereas areas with water-saturated sandy soils face the risk of liquefaction. Conducting a geological survey to examine the soil composition is crucial for identifying the potential risks associated with these secondary post-earthquake events.

The southern coastal area predominantly comprises kurkar rock, a relatively young geological formation that has not experienced significant geological upheavals. This lack of historical geological stress means the kurkar has yet to undergo extensive compaction, crystallization, or fossilization processes that typically strengthen older rocks. As a result, the kurkar in this region exhibits a different level of cohesion and resistance to weathering than observed in the more mature rock formations along the cliffs of Rosh HaNikra and other northern coastal parts of the country. This area is also affected by the dynamic processes of wave erosion and sand drift, further influencing the geological stability and response to seismic events.

2.2.1. Soil Liquefaction

Liquefaction occurs when water-saturated, loose granular sediments lose strength and act as a liquid under seismic shaking. This phenomenon happens due to a sudden increase in pore water pressure within the sediment during an earthquake, weakening the grain-to-grain contacts and causing the sediment to behave fluidly [25,26]. Consequently, heavy infrastructure may sink into the liquefied ground, while lighter structures might rise or float. The likelihood of liquefaction is influenced by several factors, including the grain size distribution, density, clay content, mineralogy, the depth of the groundwater table, and the characteristics of the earthquake's ground motion, such as its magnitude and duration. These last two factors, reflecting the seismic vibrations and the site's proximity to the earthquake source, are particularly crucial in assessing liquefaction risk. Risk levels for liquefaction are determined using hazard maps developed by the Geological Survey of Israel [27] (see Figure 1 at the top right). It is important to note that, unlike the guaranteed impact of seismic shaking in an earthquake, the potential for liquefaction under the above conditions remains uncertain, with no guarantee that it will occur.

2.2.2. Slope Stability

Landslides and rock falls, triggered by factors such as earthquakes or heavy rainfall, are driven by gravity and can lead to catastrophic consequences, particularly in populated areas, by causing significant damage and loss of life yearly [28–31]. These downslope movements of material are classified based on their nature into slides, where an intact mass of material moves cohesively; flows, which occur when materials, usually with high water content, move similarly to viscous fluid; and creep, characterized by the very slow, often imperceptible movement of material. Additionally, rock falls occur when fractured rock masses on steep slopes break apart, causing rock blocks to detach and fall. The specific type of movement is determined by the interaction between the material's mechanical characteristics and the external forces acting on it, such as gravity and seismic activities. The work of Maina-Gichaba et al. [32] emphasizes the importance of recognizing factors such as location, human activity, and the frequency of such events to mitigate their impact. Effective mitigation strategies involve several key actions: first, avoiding construction in areas known to be high-risk; second, implementing strict land-use policies to manage development; third, enhancing public awareness about the risks associated with landslides; and, finally, obtaining professional engineering evaluations to assess and mitigate potential hazards accurately. The authors suggest construction practices that minimize risk, such as avoiding steep slopes, stabilizing slopes through groundwater management, and using retaining structures. Furthermore, in the Israeli context, the Geological Survey of Israel [33] uses slope stability sensitivity maps to assess hazard risk levels (see Figure 1 on the right

bottom), focusing on potential slope failures and emphasizing the complex relationship between geological phenomena and the need for targeted mitigation efforts. Additionally, studies such as those by [34,35] have explored specific failure mechanisms, including the collapse of concrete separation walls due to soil pressure.

2.2.3. Amplitudes of Seismic Waves

Recent research has illuminated that specific site conditions can significantly amplify seismic wave intensity and increase damage during earthquakes [36–39]. The primary factor influencing a site's response is the structure of the shallow subsurface rock layers, especially when soft rock layers with low seismic velocities overlay hard rock layers with high seismic velocities. This geological configuration can lead to resonance in the soft upper layer, enhancing the seismic waves' intensity and delaying their decay. Deep and narrow basins in the subsurface and specific topographies such as mountainous or cliff areas contribute to the intensity of seismic vibrations. However, this work does not cover their risk assessment and the development of mitigation due to a lack of information on these factors.

This knowledge facilitates the early identification of areas at risk for seismic vibration amplification through subsurface geology and local topography analyses. Consequently, qualitative and quantitative risk maps can be produced based on available data on the geotechnical and seismic properties of the rock layers and predictive models. Nevertheless, conducting a precise quantitative evaluation of risk levels for this and other factors requires a detailed study at a specific site.

Risk levels related to this amplification factor are delineated in the Israeli Standard 413 [23,24], drawing from a map identifying areas prone to exceptional site amplification (see Figure 1 at the middle top).

2.3. Tsunami

Tsunami impacts vary from minor to catastrophic, heavily influenced by the magnitude and location of the initiating earthquake. Although “mega-tsunamis” lack a precise scientific definition, they are known for their profound socio-economic consequences. A notable example is the 2004 Indian Ocean Tsunami, which, according to the NGDC/WDS Tsunami Event Database, resulted in nearly 230,000 deaths across various nations following a magnitude (M) 9.1 earthquake. This incident and others, such as the 2011 Tohoku Tsunami, highlight the catastrophic potential of such natural phenomena. The Tohoku Tsunami in 2011 claimed 15,893 lives in Japan and led to significant economic damages throughout the Pacific, affecting places as far as California, as documented by Ewing (2011) [40]. Moreover, the 20th century's most potent earthquake, the 1960 Chile Earthquake (moment magnitude of 9.5), triggered tsunamis that inflicted considerable destruction and loss of life in Hawaii. Between these notable incidents, various significant tsunami events have further illustrated their widespread occurrence and diverse impacts worldwide. For example, the 1964 M 9.2 Great Alaskan Earthquake caused tsunamis that resulted in 122 fatalities and inflicted damages estimated between USD 300 and USD 400 million in Alaska alone, as reported by NOAA (2017) [41].

In response to the continual risk caused by tsunamis, the Federal Emergency Management Agency (FEMA) [42] has developed the Hazus Tsunami Loss Estimation Methodology. This tool aims to estimate the potential consequences of a tsunami event on a coastal city, county, or region, providing insights into the possible scale and extent of damage and disruption. The methodology delivers key outputs, including quantitative estimates of direct repair and replacement costs, costs associated with loss of function such as business revenue and relocation, and casualties. It also assesses functionality losses, including the loss of function and restoration times for specific facilities.

Utilizing Geographic Information Systems (GIS)-based software, Hazus facilitates detailed studies across diverse geographic scales and population densities, making it accessible to a broad spectrum of users. The methodology incorporates baseline inventory

data, such as classification systems for the General Building Stock (GBS), demographic, and economic data, alongside standard [43–45] calculations for estimating the type and extent of damage. National and regional databases provide baseline data for those without user-supplied information. This integration allows Hazus to support varying complexity levels in estimates, depending on the detail of inventory data provided, with more detailed data yielding more accurate results.

Aimed at High to Very High Tsunami Risk States and US territories as identified by the National Tsunami Hazard Mitigation Program (NTHMP), this evolving methodology emphasizes the need for a modern approach to disaster risk management. It highlights the importance of preparedness and informed decision making in mitigating future tsunami impacts, aiding in developing recovery plans, and anticipating emergency responses. The comprehensive approach taken by the Hazus Tsunami Loss Estimation Methodology in estimating tsunami impacts showcases the significance of integrating advanced modeling techniques with practical disaster management strategies, underlining the critical need for comprehensive understanding and preparedness to minimize the effects of tsunamis worldwide (see Figure 1 left bottom for world map of historical tsunami sources).

3. Methodology

The research methodology is composed of four main phases. The flowchart of the methodology is illustrated in Figure 2.

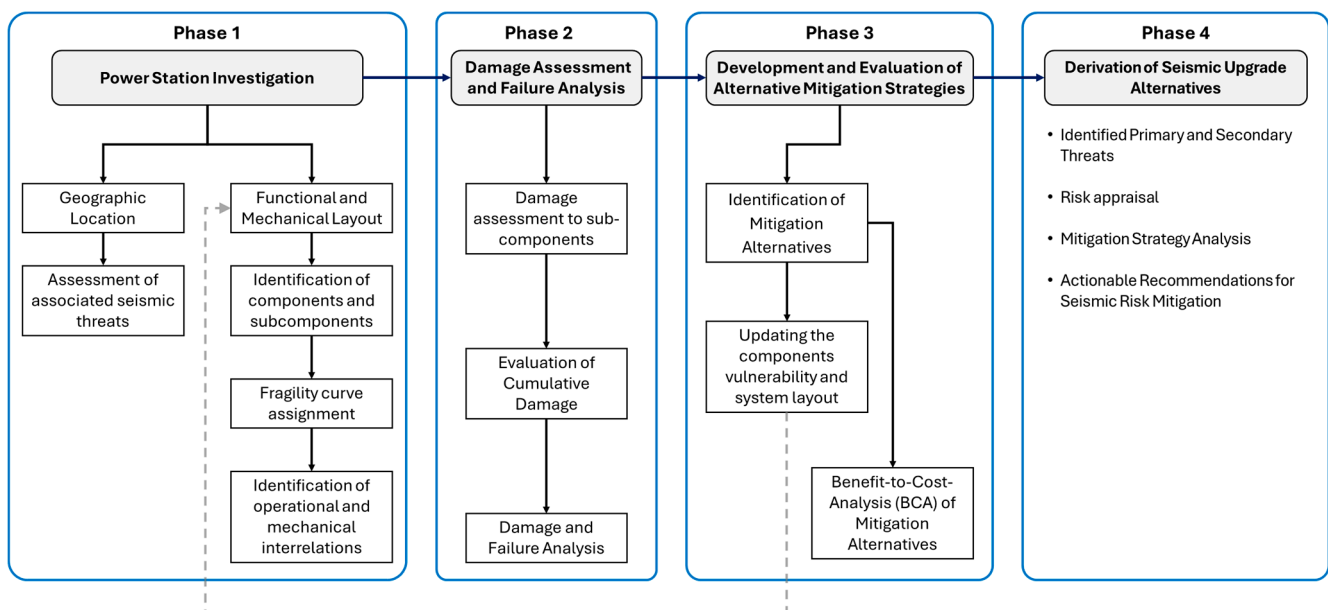


Figure 2. Main phases of the methodology.

3.1. Phase 1—Investigation of the Power Station

This phase establishes a thorough understanding of the power station’s configuration. The objectives are to pinpoint the geographic location and the associated seismic risk, identify the primary components and the subcomponents, and characterize their mechanical and operational interdependencies.

Power Station Location

Detailed geographic and seismic zoning are established, forming the basis for evaluating potential seismic risks. The location serves as a critical factor in determining the risk exposure. The detailed analysis is based on the location of the power station and consideration of site effects.

Assessing seismic threats and their occurrence probabilities involves analyzing the likelihood and potential severity of seismic risks associated with the power station’s

geographic location. The assessment categorizes the threats into primary earthquake events and secondary seismic events.

1. **Primary Earthquake Event**—it is crucial to identify the occurrence probabilities of earthquake events and their associated ground motion at the site. Hazard maps and other available data, such as historical seismic records or local geological surveys, can support this step. If required, probabilistic seismic hazard analysis (PSHA) models may be employed to quantify the likelihood of earthquakes impacting the power station, considering factors such as fault locations, seismic activity rates, and ground motion attenuation [46].
2. **Secondary Seismic Events**—review of possible subsequent events that can be triggered as a result of the earthquake, such as:
 - **Amplification**—evaluating the soil and geological conditions to determine the site’s susceptibility to seismic amplification.
 - **Slope Stability**—assessing the probability of landslides and slope failure due to seismic shaking.
 - **Liquefaction**—analyzing soil liquefaction potential based on soil composition, groundwater levels, and historical liquefaction occurrences.
 - **Tsunami**—determination of the occurrence probability and characteristics of tsunami events, utilizing historical data, simulations, and other pertinent information.
 - **Power station structure and vulnerability.**

Structural and Component Analysis—the power station structure and layout must be thoroughly investigated to identify the facility’s main components and subcomponents. Additionally, this step must include the determination of the functional and mechanical interdependencies between components and establishing how the failure of one could affect another. This step also includes the functionality investigation of the components in routine and emergency conditions.

Components Vulnerability definition—fragility curve parameters are identified and associated with each essential component and subcomponent within the system. These parameters are typically obtained from established sources such as the Hazus technical manual [47] and the FEMA database [48] or previous research [49–51]. However, in cases where suitable fragility curves are unavailable, this step may be supported by collaboration with structural engineers, alongside the utilization of historical damage data, empirical studies, and analytical models [52,53], or by the development of specific fragility curves [54,55].

3.2. Phase 2—Damage Assessment and Failure Analysis

This phase aims to quantitatively evaluate the potential damage to the power station’s components and subcomponents as a result of the primary earthquake event and secondary events. This phase is based on the threats and the system layout defined in the previous phase.

- **Subcomponent Damage Assessment**—the predicted ground motion at the power station site is applied to the fragility curves in order to calculate the probability and severity of damage to each subcomponent.
- **Cumulative Damage Evaluation**—aggregation of damage accumulated from the primary and secondary events to assess the overall cumulative damage sustained by the subcomponents.
- **Damage and Failure Analysis**—a comprehensive failure analysis is conducted, considering the interdependencies between components and the system’s redundancy and resilience. Fault Tree Analysis (FTA) is utilized to provide an in-depth evaluation of failure modes and their implications.

3.3. Phase 3—Alternative Mitigation Strategies Evaluation

In this phase, alternative mitigation strategies are identified and evaluated to address the seismic risks outlined in previous phases. The assessment incorporates adjustments to the components' vulnerabilities and the power station's overall layout, reflecting the impact of the proposed mitigation measures.

- Mitigation alternatives identification—possible mitigation strategies are identified to enhance the power station's seismic resilience. These strategies could involve structural upgrades, system redundancies, improved emergency response plans, or other relevant measures.
- Updating the components' vulnerability and system layout—based on the mitigation strategy and measures, the vulnerability of each component and the overall system layout are re-evaluated to reflect the expected impact on seismic resilience. This step includes updating fragility parameters, adjusting the system's mechanical and functional relationships, and implementing other relevant modifications to its layout.
- Benefit-to-cost analysis—this process assesses the economic effectiveness of the proposed mitigation strategies by examining the balance between expected risk reduction and the costs of implementation. The analysis aims to evaluate each strategy's worth and identify the most cost-effective option. This process compares the anticipated benefits of a mitigation measure, in terms of reduced economic losses from earthquakes, against the estimated costs of implementation. Decision trees are employed to systematically compare and quantify the benefits and costs of alternative strategies.

3.4. Phase 4—Synthesis and Recommendations

This final phase highlights the findings from the preceding phases and turns them into actionable recommendations. It synthesizes the results of the damage assessments, failure analyses, and mitigation evaluations to provide a cohesive understanding of the power station's seismic vulnerabilities and the effectiveness of various mitigation strategies. These recommendations are intended as a decision support tool to guide the power station's decision makers in enhancing seismic resilience.

4. Case Study

In this chapter, a thorough examination of a power station is presented. However, it is important to note that, due to safety concerns, several facility specifications have been omitted from this publication.

4.1. Power Station Investigation

The power station under investigation is a natural gas-fired, combined cycle power plant located in the southern coastal plain of Israel, near the city of Ashkelon. The plant has a total generating capacity of 860 MW and plays a critical role in supplying electricity to the national grid. In normal status, the power plant is expected to produce more than 800 Megawatts for the electricity grid and an additional up to 60 Megawatts for self-use. The power station site covers a total area of 90,000 square meters and includes various facilities and infrastructure, such as natural gas receiving and processing facilities, water treatment and cooling systems, electrical switchgear and transmission infrastructure, control rooms and administrative buildings, and maintenance workshops and storage areas. The construction of the power station was completed in 2014, following a three-year construction period. The total estimated construction cost of the project was approximately USD 1.2 billion.

As a critical infrastructure asset, the power station is subject to stringent safety, security, and environmental regulations. Additionally, regular maintenance and inspection activities are carried out to maintain the reliability and performance of the power station's components and systems. Given its strategic importance, the power station has been designed and constructed in accordance with the Israeli building code (SI 413) and other relevant standards for critical infrastructure protection. However, the plant's location in a

seismically active region necessitates a comprehensive assessment of its seismic resilience and the development of appropriate mitigation strategies to ensure its continued operation and minimize the impact of potential seismic events.

4.2. The Location and Seismic Risks

The power station is located in the south of the coastal plain in Israel, near Ashkelon city. Consequently, the seismic hazard evaluation considered the existing seismic risk in this area. The seismic hazard was evaluated based on the defined risks presented by [56–58]. PGA, a parameter representing the value of ground motion at the site, was applied to assess seismic hazards. The Israeli building seismic design code (SI 413) [23], along with [56], provides PGA zone maps for Israel. These maps were developed using the Probabilistic Seismic Hazard Analysis (PSHA) methodology and provide three return periods: 2%, 5%, and 10% over 50 years. Considering the power station’s designation as critical infrastructure, a return period of 2% in 50 years was selected. In the south coastal plain region, where the power station is located, the PGA value was determined to be 0.15 g. According to the hazard scale proposed for ground shaking effects by Salamon et al. (2018) [58], a predicted PGA between 0.15 g and 0.20 g is categorized as a high hazard level (Table 1). The soil composition in the southern coastal plain area is not prone to local amplification. Furthermore, as detailed by (Salamon et al., 2014) Salamon, Netzer-Cohen, et al. (2014) [57], the site is classified as normal ground, indicating it lacks potential for local amplification. Consequently, the selected PGA value for the primary earthquake event is expected to generate a ground motion of 0.2 g at the site.

Table 1. Earthquake Hazard Scale as proposed by Salamon et al. (2018).

Level of Hazard	Relative Degree of Hazard (HGS)	Criteria
Highest	4	$PGA \geq 0.2 \text{ g}$
High	3	$0.2 \text{ g} > PGA \geq 0.15 \text{ g}$
Moderate	2	$0.15 \text{ g} > PGA \geq 0.1 \text{ g}$
Lowest	1	$PGA < 0.1 \text{ g}$

According to the slope stability analysis carried out by Katz et al. (2008) [59], which presents the sensitivity to slope failure in Israel, the southern part of the coastal plain is categorized at the lowest degrees, “I–II”. This sensitivity level is considered negligible due to the very high critical acceleration ($>0.5 \text{ g}$) required for failure. This aligns with the low slope stability risk at the power station site, attributed to the relatively flat topography of the coastal plain. The absence of significant slopes or hillsides near the site reduces the likelihood of earthquake-induced landslides or slope failures.

Regarding liquefaction risk, the coastal area is defined as having a high degree of susceptibility to liquefaction (see Table 2). This means that there is a significant risk of soil liquefaction for foundations that are shallower than 20 m in depth.

Table 2. Liquefaction Hazard Level as proposed by Salamon et al. (2018).

Level of Hazard	Relative Degree of Hazard	Criteria
Highest	4	“Unconsolidated soil” + “ $PGA \geq 0.15 \text{ g}$ ” + “shallow ($<20 \text{ m}$) ground water”; reclaimed areas; coastal area within this PGA
High	3	“Unconsolidated soil” + “ $0.10 \text{ g} \leq PGA < 0.15 \text{ g}$ ” + “shallow ($<20 \text{ m}$) ground water”; coastal area within this PGA
Moderate	2	“Unconsolidated soil” + “ $0.05 \text{ g} \leq PGA < 0.10 \text{ g}$ ” + “shallow ($<20 \text{ m}$) ground water”; coastal area within this PGA
Lowest	1	“ $PGA < 0.05 \text{ g}$ ” + “shallow ($<20 \text{ m}$) ground water”; coastal area within this PGA

The tsunami risk assessment along Israel's Mediterranean coast relies on historical data from approximately 22 events that have impacted the eastern Mediterranean shoreline, with about 10 of these affecting Israel directly. The estimated likelihood of a tsunami occurring in Israel is defined by an event with a return period of 200 years. Furthermore, the probability of a tsunami following a local earthquake escalates with the earthquake's magnitude, estimated at a 1 in 7 chance after a magnitude 6.0 earthquake and a 1 in 3 chance after a magnitude 7.0 earthquake. For the power station site in the south of the coastal plain, the maximum predicted inundation height is estimated to be 2.5 m and up to 5.0 m [57].

4.3. Power Station Structure and Vulnerability

The station consists of two units, each containing six gas turbines, six steam boilers, and one steam turbine. Other main components include a Gas Pressure Regulating and Metering Station (PRMS), a water treatment facility, diesel fuel tanks, water tanks, and Gas-Insulated Switchgear (GIS).

The seismic fragility curves of the components and subcomponents are based on the fragility parameters proposed by Hazus [60]. Furthermore, for each component, a demonstrative damage state was selected as either moderate or complete based on the component's importance to the overall system's functionality and the potential consequences of its failure. Moreover, where necessary, a further analysis with Fault Tree Analysis (FTA) was carried out for certain systems to account for their inherent redundancy and to provide a precise representation of the system's overall seismic vulnerability.

4.3.1. Water Treatment Facility

The water arriving at the facility is subjected to distillation and mineral removal processes. This treated water is then utilized to cool the turbines and compressors. The water treatment facility is constructed of a steel truss with a concrete slab foundation, with dimensions of 10 m in height, 60 m in length, and 23 m in width. Damage to the water treatment facility can result from a loss of electricity supply, damage to processing equipment (such as pumps, pipes, and membranes), and harm to chemical storage tanks. The primary subcomponents of the water treatment facility, along with their associated fragility curves, are detailed in Table 3 and depicted in Figure 3. The expected probability of damage for these subcomponents is calculated using the fragility curves for a PGA value of 0.05 g. The estimated probabilities are presented in the table.

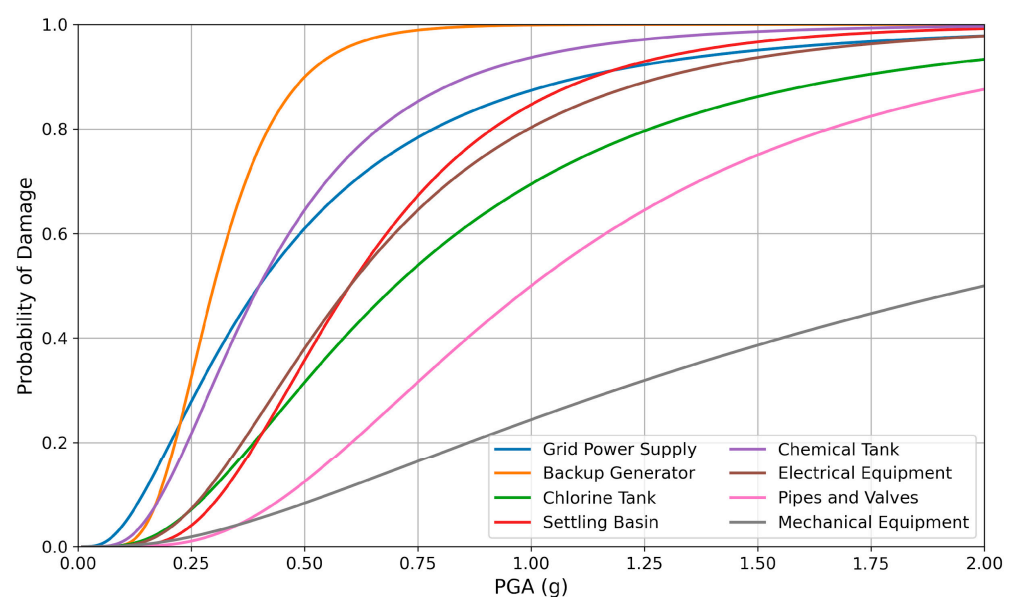


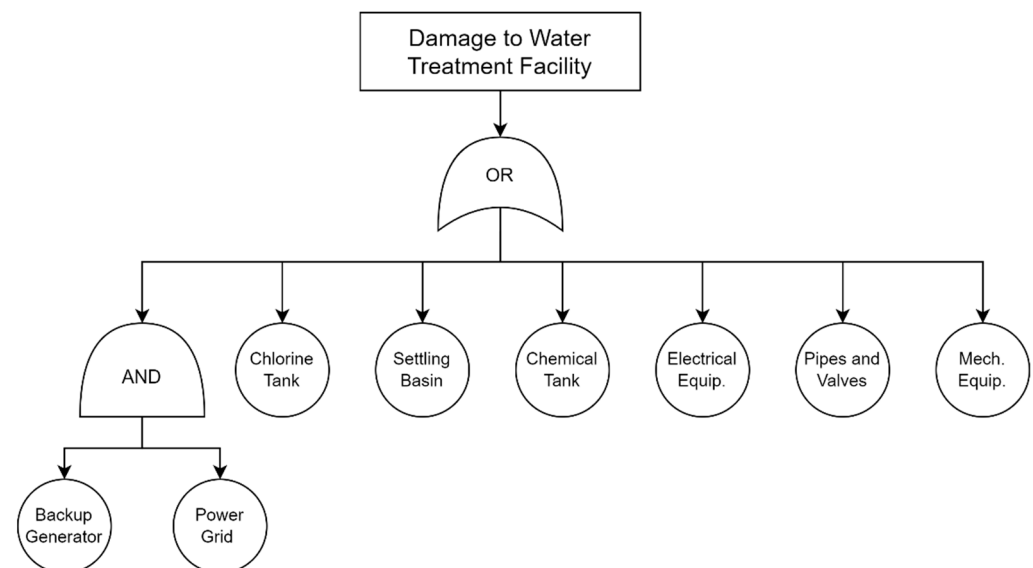
Figure 3. Fragility curves for main subcomponents of the water treatment facility.

Table 3. Subcomponents of the water treatment facility with corresponding fragility curve parameters and damage probability estimates.

Subcomponent	Median (θ)	Std (β)	Damage Probability *
Grid Power Supply	0.4	0.8	0.193
Backup Generator	0.3	0.4	0.155
Chlorine Tank	0.7	0.7	0.037
Settling Basin	0.6	0.5	0.014
Chemical Tank	0.4	0.6	0.124
Electrical Equipment	0.6	0.6	0.034
Pipes and Valves	1.0	0.6	0.004
Mechanical Equipment	2.0	1.0	0.011

* Damage probabilities are calculated based on a PGA of 0.2 g.

A Fault Tree Analysis (FTA) was conducted, utilizing the specified damage probabilities for each subcomponent. Figure 4 depicts the FTA, outlining potential failure mechanisms within the water treatment facility through “AND” and “OR” logic gates, reflecting the interdependencies among the subcomponents. The overall probability of damage to the facility was determined to be 0.231.

**Figure 4.** Fault Tree Analysis (FTA) diagram of the water treatment facility.

4.3.2. Gas Pressure Regulating and Metering Station (PRMS)

The Gas Pressure Regulating and Metering Station (PRMS) regulates and measures natural gas flow and pressure. Key components of a PRMS consist of inlet and outlet piping with associated valves, essential electrical and mechanical equipment, power sourced from the external grid complemented by a redundant backup generator, a compressor, and the encompassing structural framework. The parameters of the fragility curves for the PRMS's subcomponents are detailed in Table 4, and the fragility curves are illustrated in Figure 5. Additionally, this table includes the expected probability of damage to these subcomponents. After conducting an FTA (Figure 6), the overall probability of PRMS failure was determined to be 0.082.

Table 4. Subcomponents of the PRMS with corresponding fragility curve parameters and damage probability estimates.

Subcomponent	Median (θ)	Std (β)	Damage Probability *
Power Supply Grid	0.4	0.8	0.193
Backup Generator	0.3	0.4	0.155
Compressor	1.25	0.6	0.001
Structure	1.5	0.8	0.006
Electrical Equipment	0.6	0.6	0.034
Mechanical Equipment	2	1	0.011
Pipes and Valves	1	0.6	0.004

* Damage probabilities are calculated based on a PGA of 0.2 g.

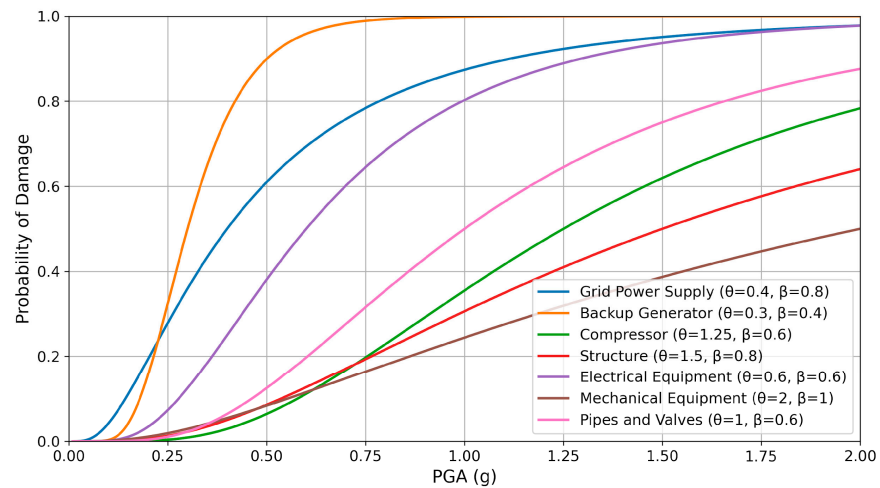


Figure 5. Fragility curves for main subcomponents of the PRMS.

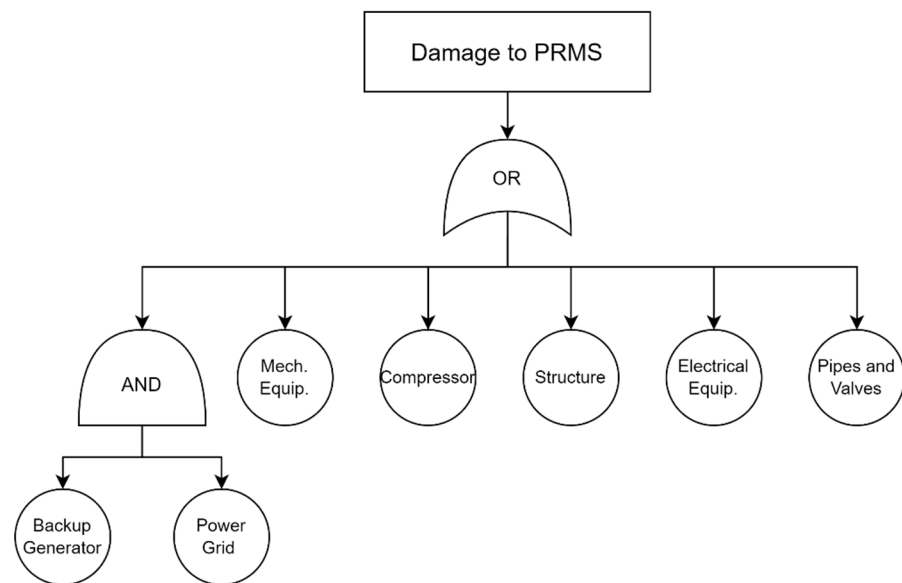


Figure 6. Fault Tree Analysis (FTA) diagram of the PRMS.

4.3.3. Gas-Insulated Switchgear (GIS)

Gas-insulated switchgear (GIS) controls and isolates high-voltage electrical equipment within gas power stations, including generators, transformers, and transmission lines, ensuring efficient and safe power distribution. A failure in the switchgear station could include a structural failure (of the building) or a failure of the electrical equipment (switches, electrical panels, transformers, and generators). Figure 7 presents the fragility curves of the

key subcomponents of the GIS, along with the fragility parameters. After conducting an FTA, the overall probability of GIS failure was determined to be 0.102.

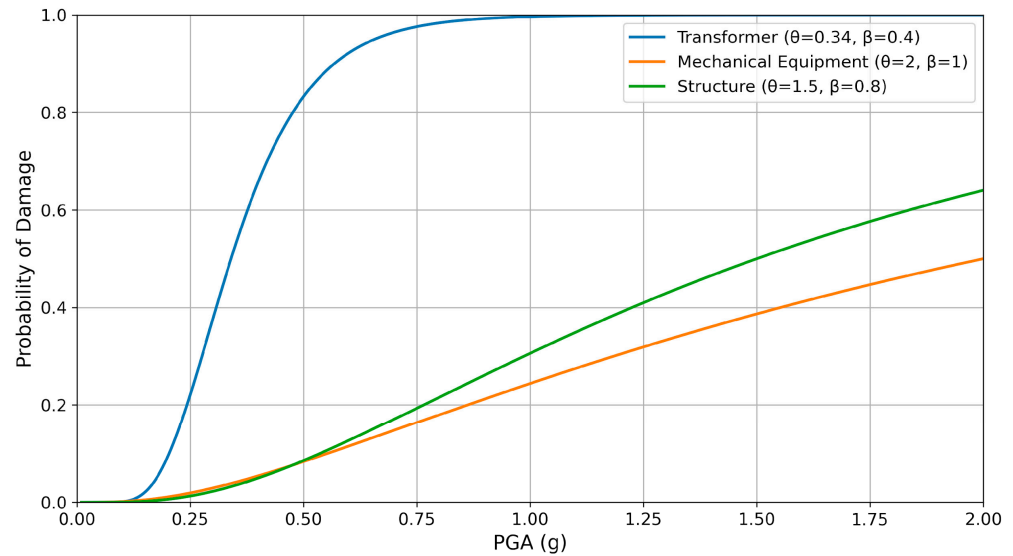


Figure 7. Fragility curves for main subcomponents of the GIS.

4.3.4. Oil and Water Tanks

The diesel storage tanks are made of steel and are founded on a concrete slab foundation. The storage tanks store diesel, which is used for power production and as a backup energy source. The steel diesel tank is 10 m high and 12.5 m in diameter. The water steel tanks store water for cooling the turbine engines, and, in an emergency, they aim to increase the pressure in the fire suppression systems. The steel water tank is 15 m high and 24 m in diameter. The diesel and water storage tanks are considered equivalent, and similar failure probabilities are attributed to them. Failure of the storage tanks may be caused by damage to critical subcomponents, such as the inlet and outlet pipelines, power supply (including both grid and backup), the on-ground steel tank, pump, and electrical and mechanical equipment. Fragility curves and fragility parameters for these subcomponents are illustrated in Figure 8. After conducting an FTA, the overall probability of tank system failure was determined to be 0.157.

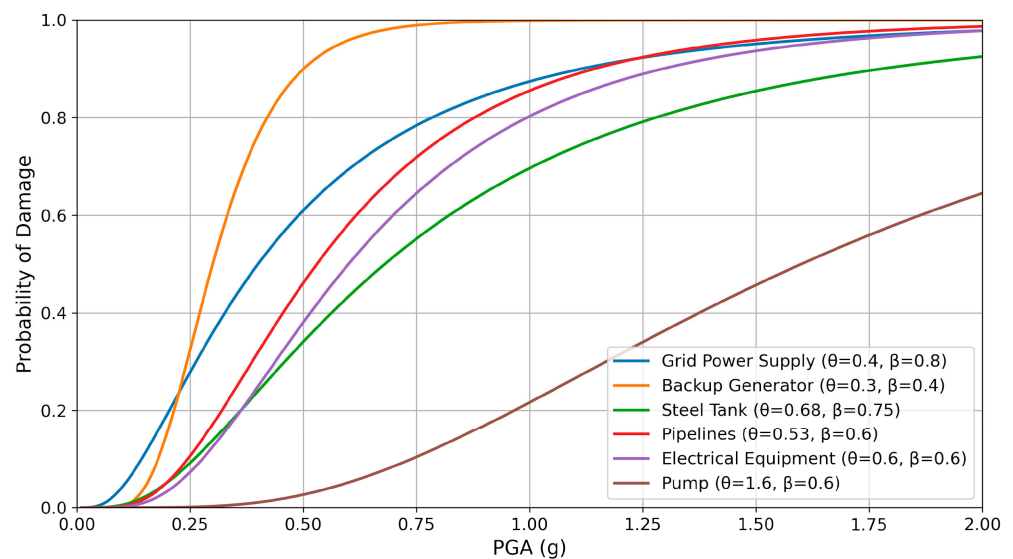


Figure 8. Fragility curves for main subcomponents of the oil and water storage tanks.

4.3.5. Steam Boilers

Each steam boiler system contains a boiler measuring 44 m in height, 28 m in length, and 26 m in width, paired with stacks extending to 80 m. These boilers and stacks, constructed from steel and set upon a concrete slab foundation, are pivotal in the station's energy production process. The station comprises 12 boilers and stacks, evenly divided between two production units, with six boilers each. The main components of the boiler system and their associated fragility curves are detailed in Figure 9.

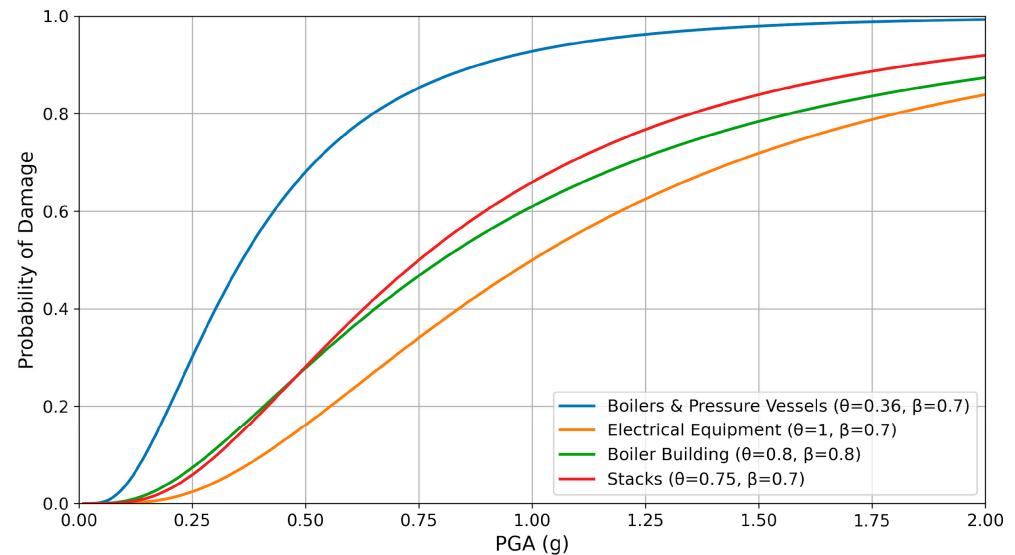


Figure 9. Fragility curves for main subcomponents of the steam boiler system.

The overall failure probability of a single steam boiler system has been determined to be 0.264. For the station to continue operating effectively, at least 8 of the existing 12 boilers must be functional. Therefore, a binomial distribution calculation was implemented to assess the likelihood of four or fewer steam boiler systems failing, ensuring the station's operational reliability. The result of this calculation determined a probability of 0.189, providing the station's operational reliability under these conditions.

4.3.6. Gas Turbines and Steam Turbines

The station has two types of turbines: a gas turbine and a steam turbine. The gas turbine spans 62 m in height, 82 m in length, and 47 m in width. Damage to the gas turbine can result from failures of the burners, air compressor, and the turbine itself. The steam turbine stands 47 m tall, extends 71 m in length, and has a width of 33 m. The condenser of the steam turbine, measuring 82 by 44 by 62, is made of steel and is placed on a raft foundation. Damage to the steam turbine may involve the transformers, generators, the turbine itself, the air compressor, or the steam condenser.

This analysis considers the probability of damage to the gas and steam turbines. The probability of damage to one turbine is determined to be 0.0416, based on fragility curve parameters specific to the turbine system by HAZUS (Figure 10). To ensure the station's continuous operation, 8 out of 12 gas turbines and both steam turbines are required to be functional. Following the binomial distribution analysis, the probability of damage is determined to be 0.0416 for the steam turbine and 7.68×10^{-5} for the gas turbines.

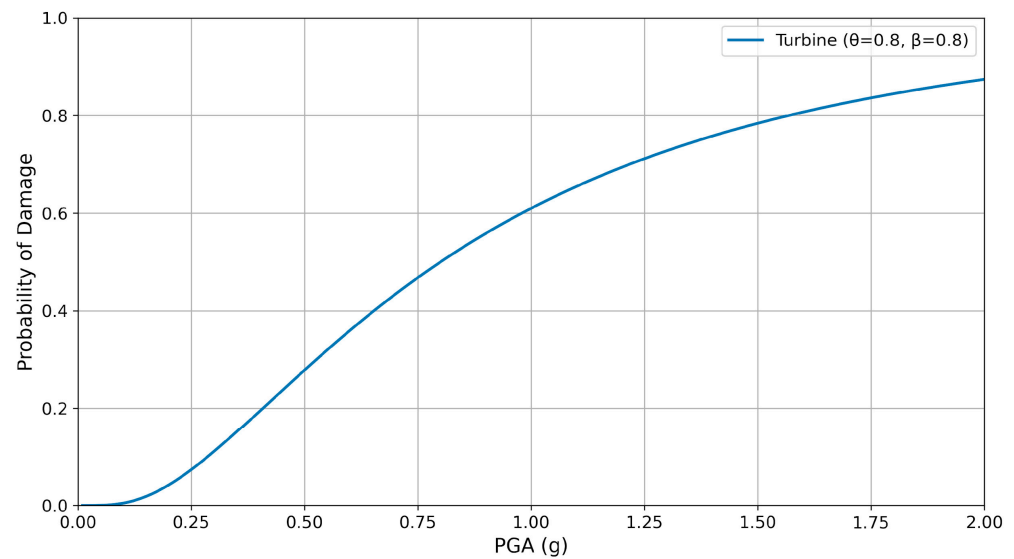


Figure 10. Fragility curves for gas and steam turbines.

4.4. Damage Assessment and Failure Analysis

The power station structure and component analysis illustrated the vulnerabilities of earthquake impacts. By employing fragility curves for various subcomponents and conducting a Fault Tree Analysis (FTA), the methodology derives the damage probabilities for the station’s main components. The summary of these damage probabilities, as detailed in Table 5, reveals varying levels of seismic vulnerability across components. The average damage probability of a component is 0.098, with a standard deviation of 0.0753, indicating the potential variability and risk distribution across the power station’s components.

Table 5. Power station main components and their determined probabilities of damage.

Power Station Component	Damage Probability *
Gas Turbines	7.68×10^{-5}
Steam Turbines	0.0416
Steam Boiler	0.0109
GIS (Gas-Insulated Switchgear)	0.1020
PRMS (Pressure Regulating and Metering Station)	0.0824
Water Treatment Facility	0.2312
Water storage Tank	0.1570
Oil storage Tank	0.1570

* Damage probabilities are calculated based on a PGA of 0.2 g.

Following the failure probabilities of the power station’s critical components, an estimate of the overall damage probability for the entire power station is achievable. A fundamental principle of this analysis is that damage to any single component, defined as significant enough to disrupt the station’s operations, contributes to the overall damage probability. For a determined PGA of 0.2 g, the total damage probability, calculated using an FTA specific to the power station, is derived to be 0.5732. It is crucial to note that this analysis treated the subcomponents as unanchored, heightening their vulnerability to seismic events, a concern that will be further discussed.

The sensitivity level for slope stability, defined as negligible, indicates that no countermeasures are required. The risk of liquefaction was identified for foundations shallower than 20 m. However, the power station was constructed in accordance with Israeli codes, which mandate conservative construction practices to safeguard and ensure the ongoing performance of critical infrastructure in regions susceptible to soil liquefaction. This means the design and construction of the power station took into account the possibility of soil liq-

uefaction, incorporating foundations deeper than 20 m to mitigate this risk. By complying with existing regulations and building codes and proactively considering the potential for soil liquefaction during the design and construction stages, the associated risks have been effectively reduced.

The tsunami scenario identified for the power station site forecasts a maximum predicted inundation height between 2.5 m and 5.0 m. To mitigate this risk, a tsunami protection wall was constructed along the perimeter of the power station. This barrier consists of precast foot wall units, each standing 9.2 m high with a base width of 3.4 m. Each unit costs approximately ILS 30,870 (around USD 8500), resulting in a total expenditure of about ILS 17 million (roughly USD 4.6 million) for the entire wall. Notably, the investment in tsunami protection represents less than 0.5% of the total construction cost of the power station, indicating a cost-effective measure to safeguard against potential tsunami impacts. This mitigation strategy highlights the practicality and cost-effectiveness of integrating protective measures against natural disasters in critical infrastructure projects. The power station significantly increases its resilience in tsunami scenarios by allocating less than 0.5% of the total construction budget to a tsunami protection wall, ensuring operational continuity and safety.

4.5. Development and Evaluation of Alternative Mitigation Strategies

Three factors are considered to quantify the risk associated with seismic events: the estimated cost of damage, the probability of an earthquake occurrence, and the total probability of damage, given that an earthquake has occurred. The *risk* is calculated using the following general equation:

$$Risk = C \times P(EQ) \times P(D|EQ) \quad (1)$$

where C represents the estimated cost of damage, $P(EQ)$ represents the probability of exceedance (i.e., the probability of an earthquake occurring), and $P(D|EQ)$ represents the probability of damage, given that an earthquake has occurred. To evaluate the estimated cost of damage, this analysis follows the structural repair cost ratio for heavy industrial facilities, using a value of 15.7% for complete damage, in accordance with the Hazus Technical Manual [47]. This percentage reflects the relative cost of repairs compared to the total replacement cost of the facility.

In our case, the estimated cost of damage to the power station due to an earthquake is USD 188.4 million, based on the construction cost of USD 1.2 billion. The probability of exceedance is calculated by considering the probability of exceeding a PGA of 0.2 g, which is determined to be one in 2475 years. For critical infrastructures, a design life cycle of 120 years is typically used, and the probability of exceedance for this duration is calculated to be 4.85%. When considering a design life cycle of 50 years, the probability of exceedance is found to be 2.02%. As found in the previous chapter, the probability of damage for a given earthquake that generated a PGA of 0.2 g at the site is 0.573 (57.3%). Therefore, the risk for a 120-year life cycle is estimated to be approximately USD 5.23 million and for a lifespan of 50 years is USD 2.18 million.

A possible mitigation strategy is anchoring the subcomponents of the power station. Anchoring reduces the vulnerability to seismic events, which is expressed by updated fragility parameters for the relevant subcomponents. Table 6 presents the updated probability of damage for a PGA of 0.2 g, calculated after updating the parameters and conducting an FTA. For anchored subcomponents, the average damage probability is 0.0397 and the standard deviation is 0.036. After conducting an FTA, the total probability of damage for the power station in the anchored condition at a PGA of 0.2 g is determined to be 0.2733 (or 27.33%).

Table 6. Damage probabilities for power station components in unanchored and anchored conditions.

Power Station Component	Damage Probability	
	Unanchored	Anchored
Gas Turbines	7.68×10^{-5}	7.68×10^{-5}
Steam Turbines	0.0416	0.0416
Steam Boiler	0.0109	0.0109
GIS (Gas-Insulated Switchgear)	0.1020	0.0360
PRMS (Pressure Regulating and Metering Station)	0.0824	0.0130
Water Treatment Facility	0.2312	0.0893
Water storage Tank	0.1570	0.0620
Oil storage Tank	0.1570	0.0620
Average	0.0978	0.0394
Standard Deviation	0.0753	0.0360
Power Station Total Probability of Damage	0.5732	0.2733

Based on the updated calculations, the risk assessment for the power station can be updated to reflect the reduced probability of damage when the subcomponents are anchored. The risk for the anchored condition is determined to be USD 2.53 million considering a 120-year life cycle and USD 1.05 million for a 50-year lifespan. This reduction represents a mitigation of 52% of the risk, which amounts to USD 2.7 million and USD 1.12 million for the 120-year and 50-year lifespans, respectively.

In order to determine the cost-effectiveness of a mitigation strategy, it is essential to conduct a BCA. Thus, if the cost of implementation is lower than the reduction in risk expectancy, the mitigation strategy is cost-effective. In the given scenario, for a 120-year lifespan, anchoring the subcomponents reduces the risk by USD 2.7 million. Therefore, if the implementation cost of this anchoring strategy is lower than USD 2.7 million, it can be considered a cost-effective solution. Additionally, the design life cycle of the power station significantly influences the evaluation of mitigation alternatives' effectiveness. The longer the design life cycle, the more advantageous the mitigation strategy is due to the increase in cumulative risk reduction over time.

Anchoring subcomponents within critical infrastructure, like power stations, is widely recognized as a strategy to enhance seismic resilience by ensuring the physical stability of crucial equipment during earthquakes. This method significantly reduces the chance of displacement and structural damage from seismic shaking, thereby minimizing the risk of operational failures. Research indicates that anchoring effectively alleviates the stress and displacement experienced by vital components such as turbines, boilers, propane tanks, water heaters, gas cylinders, and electrical systems—essential for the continuous operation of power stations. Guidelines and case studies from the Federal Emergency Management Agency (FEMA) [47] and the National Institute of Building Sciences [61] highlight how anchoring has significantly improved structural resilience against earthquakes.

The efficacy of anchoring is supported by experimental research and evaluations following earthquakes. For instance, retrofitting older structures with anchoring systems is crucial for seismic adaptation in earthquake-susceptible areas such as California and Japan [62,63]. Results from these areas indicate that anchored buildings sustain less severe damage than those without retrofitting. Additionally, the American Society of Civil Engineers (ASCE) and the Earthquake Engineering Research Institute (EERI) have extensively documented the benefits of anchoring, presenting empirical evidence that effective implementation of anchoring enhances the longevity and stability of critical infrastructures during and after seismic events [64–66].

4.6. Case Study Summary

This case study presented a risk analysis of a gas power station located in the southern coastal plain of Israel, near Ashkelon city. The seismic hazard evaluation was determined for a return period of 2% in 50 years, and the predicted PGA for the primary earthquake

event at the site is expected to be 0.2 g. Further investigation reveals that the power station is located in an area with a high degree of susceptibility to liquefaction for foundations shallower than 20 m. However, the design of the power station considered this, and the construction included deeper foundations. The estimated likelihood of a tsunami occurring at the site is an event with a return period of 200 years, with a maximum predicted inundation height between 2.5 m and 5.0 m. In order to mitigate this risk, a perimeter tsunami wall was constructed, with a total cost of 0.5% of the total construction cost. A possible mitigation strategy was proposed by anchoring critical subcomponents in the power station. The analysis illustrated that anchoring of critical subcomponents can significantly reduce the probability of damage during a seismic event. The strategy will be considered cost-effective if the implementation cost is lower than USD 2.7 million in the case of a 120-year lifespan consideration and lower than USD 1.12 million for a 50-year lifespan.

4.7. Guidelines and Recommendations

In this section, we provide comprehensive guidelines and actionable recommendations to enhance the seismic resilience of power stations, addressing the specific needs of engineers and designers involved in the construction and retrofitting of critical infrastructure:

Seismic risk assessment:

- Conduct detailed seismic risk assessments using updated geological data and advanced modeling techniques to identify potential seismic hazards specific to the location of the power station. This assessment includes evaluating fault lines, soil composition, and historical earthquake data.

Design recommendations:

- Design critical components with enhanced seismic standards that exceed the minimum code requirements to ensure robustness against higher magnitude earthquakes.

Anchoring and retrofitting:

- Implement anchoring solutions for all critical machinery and equipment to withstand the region's anticipated seismic forces.
- Use high-quality, durable materials for anchoring to improve longevity and effectiveness.
- For existing structures, conduct thorough inspections to identify vulnerabilities and retrofit them with modern anchoring techniques to improve their seismic resilience.

Isolation systems:

- Employ advanced base isolation systems and vibration control technologies to decouple the structure from the ground motion, significantly reducing the impact of seismic waves.

Monitoring and maintenance:

- Install state-of-the-art seismic monitoring systems to provide real-time data on structural integrity during and after earthquakes.
- Routine maintenance schedules to inspect and maintain seismic mitigation equipment, ensuring all components function correctly and adhere to safety standards.

Emergency response planning:

- Develop comprehensive emergency response plans that include evacuation routes, communication protocols, and recovery strategies to minimize downtime and ensure safety.
- Train staff regularly on these plans to ensure everyone knows their role during and after an earthquake.

Collaboration with Experts:

- Engage with seismic experts, structural engineers, and researchers to stay updated on the latest advances in earthquake engineering and integrate these innovations into the design and maintenance of power stations.

Regulatory compliance:

- Ensure all designs and modifications meet or exceed local and international building codes and standards related to seismic safety.
- Work with regulatory bodies to update and improve seismic standards based on the latest research and post-earthquake assessments.

5. Discussion

This research presents a comprehensive framework for evaluating and enhancing the seismic resilience of critical infrastructure. A case study of a gas power station in Israel demonstrated the implementation of this framework. The findings of the study further highlight the importance of seismic risk assessment and risk management utilizing benefit-to-cost analysis to evaluate economic efficiency.

The proposed methodology conducts an in-depth analysis of the seismic vulnerabilities of the facility's main components and subcomponents. By thoroughly examining the facility's main components and their constituent subcomponents, this approach enables a comprehensive assessment of the system's vulnerabilities and identifies targeted retrofitting measures to enhance overall resilience. This approach not only emphasizes the necessity of thoroughly examining both primary system components and their subcomponents but also requires a comprehensive understanding of their operational interdependencies. Similar approaches have been endorsed in previous studies by [11,17], demonstrating the critical value of integrated approaches to infrastructure resilience.

The results of this study show the significance of seismic retrofitting through anchoring subcomponents. This strategy decreases damage probability from 57.32% to 27.33%. Anchoring demonstrates strategic risk management and expresses the intersection of operational functionality and safety enhancements. This outcome aligns with the findings of [67,68], who have similarly documented the positive impact of anchoring on reducing seismic risk.

This study presents cost-effective seismic resilience strategies. The calculated investment in tsunami protection and critical subcomponent anchoring demonstrates the study's need to balance fiscal responsibility with critical infrastructures' integrity. This equilibrium is essential when considering the sustainability of large-scale infrastructure projects, especially given the potential impacts of climate change on the frequency and severity of natural disasters.

The case study results underscore the importance of integrating cost-benefit considerations into seismic risk management for critical infrastructure. While technical engineering assessments are crucial for identifying vulnerabilities and devising mitigation solutions, evaluating the economic feasibility of these strategies is also essential to inform decision making. Benefit-to-cost analysis (BCA) provides a systematic framework for quantifying the financial trade-offs involved in earthquake resilience investments. It enables a direct comparison of the economic effectiveness of different mitigation alternatives, which is invaluable for prioritizing limited resources and justifying resilience expenditures to stakeholders. This approach effectively bridges the gap between engineering solutions and financial constraints.

Furthermore, we suggest a strategic phased retrofitting plan to address challenges regarding anchoring. Such suggestions include selecting vulnerable components and scheduling retrofitting during low-demand periods or allowing for partial shutdowns, which can significantly mitigate disruptions. Advanced diagnostic tools and innovative construction technologies, such as modular anchoring systems and self-drilling anchors, can optimize retrofitting processes while minimizing the impact on operations.

However, it is essential to recognize the limitations of this comprehensive analysis and guide future research directions as follows:

- The case study focuses on a gas power station located in Israel. Given the unique seismic and geotechnical characteristics of the region, the findings may not be directly applicable to other geographical locations. Therefore, future studies should consider a

diverse set of geographical locations, including those with different seismic profiles and infrastructure types. Comparative studies across various regions could help generalize the findings and develop more universally applicable resilience strategies.

- The study does not account for the impact of aftershocks, which can lead to cumulative damage and affect the resilience and recovery of infrastructure following the primary earthquake event [69]. Future research could enrich the methodology with the analysis of aftershocks in seismic risk assessments.
- This research did not account for additional factors affecting seismic vulnerability, such as proper maintenance, the age of the facility, and the surrounding environment. Future research should integrate a broader set of parameters into the seismic risk assessment methodology as was presented by [70]. Adopting such an expanded approach will enhance the comprehensiveness and accuracy of evaluations, leading to more effective mitigation and preparedness strategies.

6. Conclusions

This study's detailed analysis of a gas power station underlines the critical importance of seismic resilience in critical infrastructure, revealing both vulnerabilities to extreme seismic events and effective mitigation strategies. The essential findings associated with the mitigation measures discussed are as follows:

- The study utilized fragility curves and FTA to evaluate the seismic vulnerabilities across the power station's components, demonstrating varying levels of risk with an average damage probability of 0.098 and a standard deviation of 0.0753.
- Anchoring subcomponents significantly reduced the overall damage probability from 57.32% to 27.33%, highlighting the effectiveness of retrofitting strategies in mitigating seismic risks.
- Despite the risk of soil liquefaction for foundations shallower than 20 m, the power station's construction followed Israeli codes, incorporating foundations deeper than 20 m to reduce associated seismic-induced liquefaction risks effectively.
- The construction of a tsunami protection wall, costing less than 0.5% of the total construction budget, demonstrates a cost-effective investment in protecting against tsunami impacts, enhancing the station's resilience without significant financial burden.
- The mitigation strategies employed, including the tsunami protection wall and the anchoring of subcomponents, ensure the operational continuity and safety of the power station in the face of natural disasters, underscoring the importance of proactive planning and implementation in critical infrastructure projects.

Author Contributions: Conceptualization, I.M.S., A.U. and G.L.S.; methodology, I.M.S., G.L.S. and A.U.; software, A.U. and S.M.; validation, I.M.S., G.L.S. and A.U.; formal analysis, S.M. and A.U.; investigation, S.M., G.L.S. and A.U.; resources, I.M.S.; data curation, S.M. and A.U.; writing—original draft preparation, G.L.S. and A.U.; writing—review and editing, I.M.S.; visualization, A.U. and S.M.; supervision, I.M.S.; project administration, I.M.S.; funding acquisition, I.M.S. All authors have read and agreed to the published version of the manuscript.

Funding: This research received no external funding.

Institutional Review Board Statement: Not Applicable.

Informed Consent Statement: Not Applicable.

Data Availability Statement: The raw data supporting the conclusions of this article will be made available by the authors on request.

Conflicts of Interest: The authors declare no conflict of interest.

References

1. Observatory Cumbria Intelligence. *Cumbria Floods November 2009: An Impact Assessment*; Cumbria Intelligence Observatory Carlisle: Carlisle, UK, 2010.
2. Urlainis, A.; Ormai, D.; Levy, R.; Vilnay, O.; Shohet, I.M. Loss and Damage Assessment in Critical Infrastructures Due to Extreme Events. *Saf. Sci.* **2022**, *147*, 105587. [[CrossRef](#)]
3. Cinar, E.N.; Abbara, A.; Yilmaz, E. Earthquakes in Turkey and Syria-Collaboration Is Needed to Mitigate Longer Terms Risks to Health. *BMJ* **2023**, *380*, 559. [[CrossRef](#)] [[PubMed](#)]
4. Forzieri, G.; Bianchi, A.; Silva, F.B.E.; Marin Herrera, M.A.; Leblois, A.; Lavallo, C.; Aerts, J.C.J.H.; Feyen, L. Escalating Impacts of Climate Extremes on Critical Infrastructures in Europe. *Glob. Environ. Chang.* **2018**, *48*, 97–107. [[CrossRef](#)] [[PubMed](#)]
5. Krausmann, E.; Cruz, A.M. Impact of the 11 March 2011, Great East Japan Earthquake and Tsunami on the Chemical Industry. *Nat. Hazards* **2013**, *67*, 811–828. [[CrossRef](#)]
6. Woods, D.D. Four Concepts for Resilience and the Implications for the Future of Resilience Engineering. *Reliab. Eng. Syst. Saf.* **2015**, *141*, 5–9. [[CrossRef](#)]
7. Bruno, M.; Clegg, R. A Foresight Review of Resilience Engineering. *Lloyd's Regist. Found. Rep. Ser.* **2015**. [[CrossRef](#)]
8. Rus, K.; Kilar, V.; Koren, D. Resilience Assessment of Complex Urban Systems to Natural Disasters: A New Literature Review. *Int. J. Disaster Risk Reduct.* **2018**, *31*, 311–330. [[CrossRef](#)]
9. The Rockefeller Foundation, City Resilience Framework. *Rockefeller Found. ARUP* **2014**, 928.
10. Yang, Z.; Barroca, B.; Weppe, A.; Bony-Dandrieux, A.; Laffr chine, K.; Daclin, N.; November, V.; Omrane, K.; Kamissoko, D.; Benaben, F.; et al. Indicator-Based Resilience Assessment for Critical Infrastructures—A Review. *Saf. Sci.* **2023**, *160*, 106049. [[CrossRef](#)]
11. Urlainis, A.; Shohet, I.M. Seismic Risk Mitigation and Management for Critical Infrastructures Using an RMIR Indicator. *Buildings* **2022**, *12*, 1748. [[CrossRef](#)]
12. Fei, Z.; Guo, X.; Odongo, J.O.; Ma, D.; Ren, Y.; Wu, J.; Wang, W.; Zhu, J. A Seismic Fragility Assessment Method for Urban Function Spatial Units: A Case Study of Xuzhou City. *Sustainability* **2023**, *15*, 8022. [[CrossRef](#)]
13. Mogheisi, M.; Tavakoli, H.; Peyghaleh, E. Probability Assessment of the Seismic Risk of Highway Bridges with Various Structural Systems (Case Study: Tehran City). *Sustainability* **2023**, *15*, 9783. [[CrossRef](#)]
14. Rota, M.; Zito, M.; Dubini, P.; Nascimbene, R. On the Use of Accelerometric Data to Monitor the Seismic Performance of Non-Structural Elements in Existing Buildings: A Case Study. *Buildings* **2023**, *13*, 2651. [[CrossRef](#)]
15. Maidi, M.; Lifshitz Sherzer, G.; Gal, E. Enhancing Ductility in Carbon Fiber Reinforced Polymer Concrete Sections: A Multi-Scale Investigation. *Comput. Concr.* **2024**, *33*, 385–398. [[CrossRef](#)]
16. Shafieezadeh, A.; Burden, L.I. Scenario-Based Resilience Assessment Framework for Critical Infrastructure Systems: Case Study for Seismic Resilience of Seaports. *Reliab. Eng. Syst. Saf.* **2014**, *132*, 207–219. [[CrossRef](#)]
17. Espinoza, S.; Poulos, A.; Rudnick, H.; De La Llera, J.C.; Panteli, M.; Mancarella, P. Risk and Resilience Assessment with Component Criticality Ranking of Electric Power Systems Subject to Earthquakes. *IEEE Syst. J.* **2020**, *14*, 2837–2848. [[CrossRef](#)]
18. Messore, M.M.; Capacci, L.; Biondini, F. Life-Cycle Cost-Based Risk Assessment of Aging Bridge Networks. *Struct. Infrastruct. Eng.* **2020**, *17*, 515–533. [[CrossRef](#)]
19. Forcellini, D. A Novel Methodology to Assess Seismic Resilience (SR) of Interconnected Infrastructures. *Appl. Sci.* **2022**, *12*, 12975. [[CrossRef](#)]
20. Rezvani, S.M.H.S.; Falc o Silva, M.J.; de Almeida, N.M. The Risk-Informed Asset-Centric (RIACT) Urban Resilience Enhancement Process: An Outline and Pilot-Case Demonstrator for Earthquake Risk Mitigation in Portuguese Municipalities. *Appl. Sci.* **2024**, *14*, 634. [[CrossRef](#)]
21. Garfunkel, Z.; Zak, I.; Freund, R. Active Faulting in the Dead Sea Rift. *Tectonophysics* **1981**, *80*, 1–26. [[CrossRef](#)]
22. Baker, J.; Bradley, B.; Stafford, P. *Seismic Hazard and Risk Analysis*; Cambridge University Press: Cambridge, UK, 2021; ISBN 1108604900.
23. *Israel Standard-413-3*; Designing Structural Resistance to Earthquakes. 413 Part 3. Israel Standards Institution: Tel Aviv, Israel, 1998. (In Hebrew)
24. *Israel Standard-413-5*; Designing Structural Resistance to Earthquakes. 413 Part 5. Israel Standards Institution: Tel Aviv, Israel, 1998. (In Hebrew)
25. Bayati, H.; Bagheripour, M.H. Shaking Table Study on Liquefaction Behaviour of Different Saturated Sands Reinforced by Stone Columns. *Mar. Georesources Geotechnol.* **2019**, *37*, 801–815. [[CrossRef](#)]
26. Ko, Y.Y.; Chen, C.H. On the Variation of Mechanical Properties of Saturated Sand during Liquefaction Observed in Shaking Table Tests. *Soil Dyn. Earthq. Eng.* **2020**, *129*, 105946. [[CrossRef](#)]
27. Friedman, S.; Salamon, A.; Zveibil, D.; Beton, R.; Katz, O. *Assessment of Liquefaction Potential in the Zevulun Valley: A Geotechnical Perspective*; Report GSI/09/2007; Geological Survey of Israel: Jerusalem, Israel, 2007.
28. Davies, T.C. Landslide Research in Kenya. *J. African Earth Sci.* **1996**, *23*, 541–545. [[CrossRef](#)]
29. Ngecu, W.M.; Ichang'i, D.W. The Environmental Impact of Landslides on the Population Living on the Eastern Footslopes of the Aberdare Ranges in Kenya: A Case Study of Maringa Village Landslide. *Environ. Geol.* **1999**, *38*, 259–264. [[CrossRef](#)]
30. Claessens, L.; Knapen, A.; Kitutu, M.G.; Poesen, J.; Deckers, J.A. Modelling Landslide Hazard, Soil Redistribution and Sediment Yield of Landslides on the Ugandan Footslopes of Mount Elgon. *Geomorphology* **2007**, *90*, 23–35. [[CrossRef](#)]

31. Knapen, A.; Kitutu, M.G.; Poesen, J.; Breugelmans, W.; Deckers, J.; Muwanga, A. Landslides in a Densely Populated County at the Footslopes of Mount Elgon (Uganda): Characteristics and Causal Factors. *Geomorphology* **2006**, *73*, 149–165. [[CrossRef](#)]
32. Maina-Gichaba, C.; Kipseba, E.K.; Masibo, M. Overview of Landslide Occurrences in Kenya: Causes, Mitigation, and Challenges. In *Developments in Earth Surface Processes*; Elsevier: Amsterdam, The Netherlands, 2013; Volume 16, pp. 293–314, ISBN 0928-2025.
33. Katz, A.; Almog, A. *Landslide Risk Assessment Map for Northern Israel: A Comprehensive Overview at a 1:200,000 Scale*; GSI/38/2006; Geological Survey of Israel: Jerusalem, Israel, 2006.
34. Mitelman, A.; Lifshitz Sherzer, G. Coupling Numerical Modeling and Machine-Learning for Back Analysis of Cantilever Retaining Wall Failure. *Comput. Concr.* **2023**, *31*, 307. [[CrossRef](#)]
35. Lifshitz Sherzer, G.; Grigorovitch, M.; Mitelman, A. Insights from LDPM Analysis on Retaining Wall Failure. *Comput. Concr.* **2024**, *33*.
36. Wang, S.; Hao, H. Effects of Random Variations of Soil Properties on Site Amplification of Seismic Ground Motions. *Soil Dyn. Earthq. Eng.* **2002**, *22*, 551–564. [[CrossRef](#)]
37. Wang, L.; Wu, Z.; Xia, K. Effects of Site Conditions on Earthquake Ground Motion and Their Applications in Seismic Design in Loess Region. *J. Mt. Sci.* **2017**, *14*, 1185–1193. [[CrossRef](#)]
38. Frid, M.; Kamai, R. Characterizing Nonlinear Effects in Vertical Site Response of Dry Soils Using KiK-Net Data. *J. Earthq. Eng.* **2023**, *27*, 2570–2586. [[CrossRef](#)]
39. Kamai, R.; Yagoda-Biran, G. Engineering-Oriented Ground-Motion Model for Israel. *Bull. Earthq. Eng.* **2023**, *21*, 3199–3220. [[CrossRef](#)]
40. Ewing, L. *A Preliminary Report on Effects to the California Coast and Planning Implications*; A Report to Coastal Commissioners; National Centers for Environmental Information (NCEI): Asheville, NC, USA, 2011.
41. NOAA On This Day: Great Alaska Earthquake and Tsunami. 2017. Available online: <https://www.ncei.noaa.gov/news/great-alaska-earthquake> (accessed on 10 April 2024).
42. *FEMA Hazus Earthquake Model Technical Manual*; Federal Emergency Management Agency: Washington, DC, USA, 2020; pp. 1–436.
43. *ASCE/SEI 31-03*; ASCE Seismic Evaluation of Existing Buildings. American Society of Civil Engineers: Reston, VA, USA, 2003.
44. *ASCE/SEI 7-10*; ASCE Minimum Design Loads for Buildings and Other Structures. American Society of Civil Engineers: Reston, VA, USA, 2010.
45. *ASCE Tohoku Japan Tsunami of 11 March 2011—Performance of Structures*; ASCE Monograph, American Society of Civil Engineers: Reston, VA, USA, 2012.
46. Baker, J.W. An Introduction to Probabilistic Seismic Hazard Analysis (PSHA). *Bak. Res. Gr.* **2008**, 1–72.
47. *FEMA Hazus Earthquake Model Technical Manual—Hazus 5.1*; Federal Emergency Management Agency: Washington, DC, USA, 2022; Volume 1, pp. 1–467.
48. Hamburger, R.O. FEMA P58 Seismic Performance Assessment of Buildings. In Proceedings of the NCEE 2014—10th U.S. National Conference on Earthquake Engineering: Frontiers of Earthquake Engineering, Anchorage, AK, USA, 21–25 July 2014.
49. Alliance American Lifelines (ALA). Seismic Fragility Formulations for Water Systems. 2001. Available online: https://www.americanlifelinesalliance.com/pdf/Part_1_Guideline.pdf (accessed on 10 April 2024).
50. Gehl, P.; Desramaut, N.; Réveillère, A.; Modaressi, H. Fragility Functions of Gas and Oil Networks. *Geotech. Geol. Earthq. Eng.* **2014**, *27*, 187–220.
51. O'Rourke, M.J.; So, P. Seismic Fragility Curves for On-Grade Steel Tanks. *Earthq. Spectra* **2000**, *16*, 801–815. [[CrossRef](#)]
52. Baker, J.W. Efficient Analytical Fragility Function Fitting Using Dynamic Structural Analysis. *Earthq. Spectra* **2015**, *31*, 579–599. [[CrossRef](#)]
53. Rabi, R.R.; Bianco, V.; Monti, G. Mechanical-Analytical Soil-Dependent Fragility Curves of Existing Rc Frames with Column-Driven Failures. *Buildings* **2021**, *11*, 278. [[CrossRef](#)]
54. Dabiri, H.; Faramarzi, A.; Dall'Asta, A.; Tondi, E.; Micozzi, F. A Machine Learning-Based Analysis for Predicting Fragility Curve Parameters of Buildings. *J. Build. Eng.* **2022**, *62*, 105367. [[CrossRef](#)]
55. Urlainis, A.; Shohet, I.M. Development of Exclusive Seismic Fragility Curves for Critical Infrastructure: An Oil Pumping Station Case Study. *Buildings* **2022**, *12*, 842. [[CrossRef](#)]
56. Klar, A.; Meirova, T.; Zaslavsky, Y.; Shapira, A. Spectral Acceleration Maps for Use in SI 413 Amendment No. 5. *Geophys. Inst. Isr. Jerus. Isr.* **2011**.
57. Salamon, A.; Netzer-Cohen, C.; Zilberman, E.; Amit, R. *Qualitative Evaluation of Earthquake Hazards for Archaeological and Historical Sites in Israel*; Technical Report GSI/28/2014; 2014.
58. Salamon, A.; Netzer-Cohen, C.; Cohen, M.; Zilberman, E. Preliminary Methodology for Qualitative Assessment of Earthquake Hazards to Historical Monuments in Israel. *Int. J. Disaster Risk Reduct.* **2018**, *31*, 1062–1081. [[CrossRef](#)]
59. Katz, O.; Hecht, H.; Almog, E. National Hazard Map of Slope-Failure in Israel. GSI/07/2008; 2008.
60. Federal Emergency Management Agency (FEMA). *Hazus Flood Model User Guidance*; Federal Emergency Management Agency: Washington, DC, USA, 2018.
61. GCR, N. *Development of NIST Measurement Science R&D Roadmap: Earthquake Risk Reduction in Buildings*; The National Institute of Building Sciences: Washington, DC, USA, 2013.
62. Maffei, J.R. The Seismic Evaluation and Retrofitting of Bridges. Ph.D. Thesis, University of Canterbury, Christchurch, New Zealand, 1996. [[CrossRef](#)]

63. Scholl, R.E. *Reducing Seismic Hazards of Existing Buildings*; DIANE Publishing: Collingdale, PA, USA, 1993; ISBN 1568065736.
64. Dizhur, D.; Schultz, A.; Ingham, J. Pull-Out Behavior of Adhesive Connections in URM Walls. *Earthq. Spectra* **2016**, *32*, 2357–2375. [[CrossRef](#)]
65. Zhang, K.; Fang, Z.; Nanni, A.; Hu, J.; Chen, G. Experimental Study of a Large-Scale Ground Anchor System with FRP Tendon and RPC Grout Medium. *J. Compos. Constr.* **2015**, *19*, 4014073. [[CrossRef](#)]
66. Cerato, A.B.; Victor, R. Effects of Long-Term Dynamic Loading and Fluctuating Water Table on Helical Anchor Performance for Small Wind Tower Foundations. *J. Perform. Constr. Facil.* **2009**, *23*, 251–261. [[CrossRef](#)]
67. Omidvar, B.; Azizi, R.; Abdollahi, Y. Seismic Risk Assessment of Power Substations. *Environ. Energy Econ. Res.* **2017**, *1*, 43–60.
68. Pavel, F.; Vacareanu, R. Seismic Risk Assessment for Elements of the Electric Network in Romania. *Buildings* **2022**, *12*, 244. [[CrossRef](#)]
69. Li, P.; Li, X.; Wang, X.; Wang, D. Seismic Resilience Evaluation of Reinforced Concrete Frame Considering the Effect of Mainshock-Aftershock Sequences. *Appl. Sci.* **2023**, *13*, 12620. [[CrossRef](#)]
70. Urlainis, A.; Shohet, I.M. A Comprehensive Approach to Earthquake-Resilient Infrastructure: Integrating Maintenance with Seismic Fragility Curves. *Buildings* **2023**, *13*, 2265. [[CrossRef](#)]

Disclaimer/Publisher’s Note: The statements, opinions and data contained in all publications are solely those of the individual author(s) and contributor(s) and not of MDPI and/or the editor(s). MDPI and/or the editor(s) disclaim responsibility for any injury to people or property resulting from any ideas, methods, instructions or products referred to in the content.